Impact of the Paper Degradation State and Constituents on Its Behavior During and After X-ray Exposure

Alice Gimat (alice.gimat@orange.fr)
CRC: Centre de recherche sur la conservation https://orcid.org/0000-0001-5339-4726
Sebastian Schoeder
Synchrotron SOLEIL
Mathieu Thoury
IPANEMA
Anne-Laurence Dupont
CRC: Centre de recherche sur la conservation

Research Article

Keywords: calcium carbonate, cellulose degree of polymerization, gelatin, iron gallate ink, yellowing, UV fluorescence

Posted Date: November 11th, 2021

DOI: https://doi.org/10.21203/rs.3.rs-1000597/v1

Impact of the paper degradation state and constituents on its behavior during and after X-ray exposure

Alice Gimat[1*], Sebastian Schöder[2], Mathieu Thoury[3], Anne-Laurence Dupont[1*]

[1] *Centre de Recherche sur la Conservation des Collections (CRC, CNRS USR 3224), Muséum National d'Histoire Naturelle, 36 rue Geoffroy St Hilaire 75005 Paris, France*

[2] *Synchrotron SOLEIL, 91192 Gif-sur-Yvette, France;*

[3] *IPANEMA, CNRS, Ministère de la Culture, UVSQ, USR3461, Université Paris Saclay, 91192 Gif-sur-Yvette, France;*

**corresponding authors: alice.gimat@mnhn.fr and anne-laurence.dupont@mnhn.fr*

Keywords. calcium carbonate, cellulose degree of polymerization, gelatin, iron gallate ink, yellowing, UV fluorescence.

Abstract

Paper is a complex biopolymer material which contains papermaking additives and often bears inks and other graphic media. Cultural heritage paper-based artefacts are most often deteriorated to some extent. This research explores how intrinsic factors such as constituents and degradation state can impact the modifications incurred in aged papers during and after X-ray examination. To this end laboratory model papers, artificially aged, and 18th and 19th century archival documents, with and without additives (gelatin, calcium carbonate) and iron gallate ink, were exposed to Synchrotron X-ray radiation at doses that were previously shown to incur damage in unaged cotton papers (0.7 to 4 kGy). Glycosidic scissions, hydroxyl free radicals, UV luminescence and yellowing were measured immediately after the irradiation, and were monitored over a period of three years. The depolymerization of cellulose was lower in the aged papers, as well as in the papers containing calcium carbonate and gelatin, than in the unaged fully cellulosic papers. Compared to the papers with no additives, there were more hydroxyl free radicals in the papers with calcium carbonate and slightly less in the gelatin sized papers. UV luminescence and yellowing both appeared post-irradiation, with a delay of several weeks to months, while the intensity of the responses was impacted by the various paper constituents. The papers with iron gallate ink showed limited degradation in the low doses range, most probably due to recombination of the free radicals produced. Doses below 4 kGy did not cause yellowing or UV luminescence of the archival papers within the whole monitoring period. At higher doses (26 to 36 kGy), a slight UV luminescence appeared after 21 months, as well as a slight yellowing after three years, in some of them. No clear correlation between the degradation induced by the irradiation and the constituents in the paper nor its conservation state could be made. The archival papers in good conservation state depolymerized to the same extent as the model papers, while the most degraded archival papers were less impacted than the latter.

Introduction

X-ray analytical techniques are used to examine historic documents and artworks on paper and gain insight into their materials, manufacturing techniques and history (Creagh 2007; Albertin et al. 2015; IAEA 2016; Kozachuk et al. 2016; Pouyet et al. 2017). Yet because they are ionizing, X-rays induce changes in organic (as well as inorganic) materials. Cellulose depolymerization, oxidation and changes in the optical properties have been observed under gamma-ray (Ershov 1998; Bouchard et al. 2006; Henniges et al. 2013; Bicchieri et al. 2016) and X-ray exposures (Mantler and Klikovits 2004; Kozachuk et al. 2016; Gimat et al. 2020). In quasi-pure cellulose paper, the impact of X-rays has been shown to be proportional to the dose (Gimat et al. 2020). However, due to the large diversity in the components and in the degradation state of historic cellulosic artefacts, the global impact of X-ray photons is difficult to foresee.

Paper is made of plant fibers, which besides cellulose, most often also contain other biopolymers such as hemicelluloses and lignin. Additives, fillers and sizing, are usually added to writing and drawing quality papers to enhance usability parameters: e.g. reduce water permeability, increase opacity and enhance brightness. In cultural heritage collections, such papers also often bear media such as inks and pigments. The materials and chemicals used are diverse. In ambient conservation conditions, a number of these additives can impact the paper degradation rate. For instance gelatin (Dupont 2003a) and alkaline minerals (Reissland 1999; Sequeira et al. 2006; Ahn et al. 2012; Poggi et al. 2016) have been shown to decrease the cellulose depolymerization rate, whereas transition metals in inks and pigments promote degradation by producing acids and free radicals (Selih et al. 2007; Potthast et al. 2008). If and how additives can impact the radiation-induced degradation of cellulosic paper is still unknown. The presence of absorbing elements, such as iron in the metal-gallate ink or calcium in the fillers could have a shielding effect and decrease the nominal X-ray dose, thereby lowering the degradation impact. Such a shielding effect could also be counteracted by the free radicals formed via the transition metals, which are known cellulose degradation promotors (Emery and Schroeder 1974; Jeong et al. 2014). It has been shown that iron-containing pigments undergo a redox reaction under X-ray radiation (Bertrand et al. 2015; Gervais et al. 2015; Gimat 2016). Moreover, the structural modification of an additive under irradiation can also affect the paper degradation rate. For instance, X-rays were shown to produce defects inside calcium carbonate (Kabacińska et al. 2017), whereas polypeptide chains (e.g. gelatin) were shown to

undergo hydrolysis (Moini et al. 2014). Bicchieri et al. have examined the combined impact of the degradation state and certain paper additives on the degradation incurred by ionizing radiation used for mold disinfection (Bicchieri et al. 2016). The authors used gamma-rays at a dose of 3 kGy. They tested cellulose paper Whatman n°1, as well as a commercial permanent paper (with $CaCO_3$ filler and optical brighteners, and sized with alkyl ketene dimers), which they pre-degraded by an acid treatment. The acid treated samples showed less radiation induced depolymerization than the control samples, indicating that the degradation state played a role. The permanent paper yellowed more than Whatman n°1, which was attributed to structural modifications of calcium carbonate and optical brighteners under gamma radiation. To our knowledge, such study has not been conducted using X-rays, nor at lower doses used during synchrotron X-ray examination of cellulosic cultural heritage artefacts. This lack of research motivated the present study, which attempts at better understanding the mitigated impact of X-rays on paper, depending on the fiber deterioration level and on the presence of components other than the fibers.

Handmade linen rag papers from the 18^{th} and 19^{th} century and industrially-made cotton linters papers (Whatman n°1) to which various additives were incorporated (gelatin, calcium carbonate and iron gallate ink) were exposed to synchrotron X-ray radiation. The papers, some of which had been previously artificially aged, were irradiated at doses in the range 0.7-4 kGy. The samples were characterized immediately after the exposure using a multiscale analytical procedure developed in a previous study (Gimat et al. 2020), which encompasses the macroscopic (yellowing and UV luminescence) and the microscopic scales (glycosidic scissions and formation of hydroxyl radicals). The changes were monitored over a period of three years.

Materials and Methods

Paper samples

Laboratory-prepared samples

Two types of paper were used: Whatman n°1 (W), which is a commercial paper made of cotton linters (min. 98% alpha cellulose), and a linen rag paper (R) manufactured using traditional stamper beating at Moulin du Verger papermill (Puymoyen, France). W and R were used either with no

further modification (control samples), or upon undergoing various artificial aging treatments (aged samples), in an attempt to approach the molecular degradation state of centuries old cultural heritage papers. Two artificial aging conditions, one predominantly hygrothermal (*hyg*) and the other predominantly oxidative (*ox*), were used to depolymerize and increase the carbonyl content of cellulose. The conditions were adjusted so as to achieve a similar degree of polymerization (*DP*) and a different degree of oxidation in the *hyg* and *ox* samples.

Hyg aging of W and R (samples called W_*hyg* and R_*hyg*) was performed according to the TAPPI method (TAPPI T573 sp-15 2015). Glass tubes (Wheaton, 35 mm internal diameter (ID) × 147 mm, 144 mL) were filled with 4.0 g of paper (dry weight), i.e. 4.23 g of paper conditioned at 50% relative humidity (RH) and 23 °C, based on the value of the equilibrium moisture content (EMC = 5.43 $\%_{wt}$) determined with the sorption isotherm. The tubes were hermetically closed and heated at 100 °C in an oven (Memmert UN 55 oven) during 10 days to reach a decrease in *DP* of about 50%. During *hyg* aging, both hydrolysis and oxidation occur. The weight-average degree of polymerization (DP_w) of cellulose was measured using SEC-MALS-DRI (details in Physico-chemical characterizations section) and the copper number (N_{Cu}) was determined using the standard method (TAPPI - T 430 cm-99 1999). The total carbonyl groups concentration was derived from N_{Cu} using the following formula proposed by Röhrling: $[CO] = \frac{(N_{Cu} - 0.07)}{0.06}$ (Röhrling et al. 2002). DP_w for W_*hyg* and R_*hyg* was 1490 ± 2% and 1961 ± 1.6%, respectively. N_{Cu} of W_*hyg* was 0.11.

Oxidative degradation (*ox*) was carried out by immersing W in an aqueous solution of sodium hypochlorite (0.42-0.62% active chlorine) adjusted to pH 7 with HCl 6 N, during 15 min under gentle stirring. At this pH, NaClO is known to promote enhanced carbonyl groups formation (aldehyde, ketone, and carboxyl groups) on C2, C3 and C6, short chain organic acids as well as considerable glycosidic scissions (Nevell and Zeronian 1985). The samples (called W_*ox*) were abundantly rinsed with milli-Q water until neutral pH of the water, and were dried between blotters. The DP_w for W_*ox* was 1352 ± 2% and N_{Cu} was 0.42.

Some of the W_*ox* samples additionally underwent a reduction treatment with $Na(BH)_4$ to reduce the carbonyl groups produced during the aging (aldehyde and keton functions) to alcohol groups, and achieve a nearly null N_{Cu}. To this end, a solution made with anhydrous $Na(BH)_4$ (Sigma) (2.91g) dissolved in absolute ethanol (154 mL) was prepared, in which 1.54 g of paper was immersed and left under gentle stirring during 12 hours. After reduction, the papers were

abundantly rinsed with milli-Q water until the water reached neutral pH, and were dried between blotters. The samples were called W_*red.*

A portion of the W and R control samples were sized by immersing the paper sheets in a 20 g L^{-1} aqueous solution of type B photographic grade gelatin from cattle bone (Gelita type restoration 1, Kind & Knox) at 30 °C during 10 minutes. The sheets were then dried vertically at ambient temperature. The sized samples were named W_G and R_G.

The dry gelatin uptake (UP) of W_G and R_G, determined as $UP = \frac{m_{sized\ paper\ dry} - m_{unsized\ paper\ dry}}{m_{unsized\ paper\ dry}}$, was 4.8% ± 0.2. Dry masses were calculated subtracting the EMC at 23 °C and 50% RH measured according to the standard method (TAPPI T 502 cm-07 1998). The UP value falls in the range of gelatin content in historical papers (Barrow 1972; Barrett 1992) and corresponds to a substantial amount of size in the paper (qualified as with '+' in Table 1).

Some of the W_G and R_G samples were used to apply the second compound of interest: iron gallate ink, also referred to as I (samples called W_GI and R_GI). The ink was prepared by mixing $FeSO_4$, $7H_2O$ (Sigma Aldrich, 99%) (40 g L^{-1}), gallic acid monohydrate (Sigma Aldrich, 99%) (9 g L^{-1}) and gum Arabic (Sigma Aldrich, G9752) (140 g L^{-1}). The mixture was stirred during 3 days at room temperature. The amount of gum Arabic used was purposely high in order to limit the penetration of the ink inside the paper. The iron sulfate *vs* gallic acid ratio was adapted from a recipe used in previous work (Rouchon et al. 2011). Large inked strokes (1.5 cm wide each) were applied side by side with a flat-end metal pen ("Plakat", Brause) in order to cover the whole sample surface. This procedure was not intended to replicate a quill pen stroke, but to provide a large and homogeneous inked surface (2×1 cm^2). The ink penetrated 30 to 112 microns into the paper, *i.e.* one third to one half of the sheet thickness, as observed with the optical microscope (Fig S1 in the Supplementary data file). The iron content determined by XRF using a previously established calibration curve (unpublished data) was similar in both samples: 97 (± 5) µmol g^{-1} in W_GI and 110 (±15) µmol g^{-1} in R_GI, values that are comparable to those in historical documents (36-179 µmol g^{-1}) (Rouchon et al. 2011).

The third compound added to the papers was $CaCO_3$ (samples called W_Ca). W paper was immersed in a saturated aqueous solution of calcium hydroxide (95%, Sigma Aldrich) (approx. 1.4 gL^{-1}) during 1 hour and was dried in ambient air. This was repeated four times successively in order to achieve a high calcium carbonate content. After each bath, the paper sheets were placed between

two blotters, and the excess solution was removed by applying a 10 kg Cobb test metal roller once back and forth on the blotters. Then the sheets were dried under weight. The reaction of CO_2 with the air when the paper is removed from the solution converts $Ca(OH)_2$ to $CaCO_3$, so-called alkaline reserve (AR). The AR determined according to the standard method (TAPPI T 553 om-00 2000) was 1.18 ± 0.06 mol kg^{-1}, otherwise expressed as 6.0% ± 0.3 equivalent $CaCO_3$. Additionally, a commercial permanent paper made of cotton linters, which contained 7.25% precipitated $CaCO_3$ (Krypton parchment, Spexel Inc, formerly Domtar), was used (samples named K). Because it was manually prepared, Ca distribution inside W_Ca was less homogeneous than in K paper (Fig. S2 in supplementary data file). All the samples were conditioned prior to use at 50% RH, 23 ºC according to the standard method (TAPPI T 402 sp-08 2013).

Archival papers

Five archival paper documents from the 18th and 19th century manufactured with linen rags were chosen. They were named DCN, SE, LN1, LN5, and M. They seem to have different gelatin size content, varying from light to strong, and different *DP* (Table 1 and Table S1 in the Supplementary data file). SE is a page from an 18th century printed volume and has a slightly brownish hue, which appears darker in the center inked area of the page, due to natural aging. DCN is a printed decree and has a very faint bluish hue. These two papers seem to have the lowest amount of sizing (Fig. S3 in the Supplementary data file). The three other documents (LN1, LN5 and M) are individual folios of notarial deed documents. M is a blank paper while both LN1 and LN5 are handwritten with iron gall ink. In SE, DCN, LN1 and LN5, only ink-free areas were used, in order to better compare with M. Additionally, to investigate the effect of the iron gall ink on ancient archival paper, the laboratory-made iron gallate ink was applied to some of the M samples using large strokes as previously described for papers W_GI and R_GI, which yielded a homogeneous inked area (sample called M_I).

Table 1 Samples characteristics: constituents, aging method, thickness (x), density (ρ), equilibrium moisture content (EMC) at 23 ◦C and 50% RH (TAPPI T 502 cm-07 1998), weight-average or viscometric-average (*) degree of polymerization (DP_0), pH (TAPPI T 509 om-15 2002), copper number (N_{Cu}) (TAPPI - T 430 cm-99 1999), concentration of total carbonyl groups ([CO]) (Röhrling et al. 2002), ash content (measured at 525 °C) (TAPPI 211 om-02 2002), alkaline reserve (AR) expressed as % $CaCO_3$ (TAPPI T 553 om-00 2000). Standard deviation (STD) is

provided when possible. Cot: cotton papers; lin: linen rag pulp papers; ox: oxidative degradation; hyg: hygrothermal aging; red: reduction treatment; nat. natural aging; Ca: calcium carbonate filler; I: iron gallate ink; Gel: gelatin sizing (identified with hydroxyproline spot test, with ++: highest size content; +: medium size content; ~: lowest size content (levels defined with a water drop absorption test) (Fig S3 in the Supplementary data file). n.d. stands for not determined.

Sample	**fiber**	**Additive**	**aging**	***x*** µm	***ρ*** g cm^{-3}	**EMC** % wt	***DP*$_0$**	**pH**	**N$_{Cu}$ / [CO]** µmol g^{-1}	**Ash** %	**AR** %$_{eq}$
W	cot	none	none	170	0.51	5.43	2948±2%	6.90 ±0.02	0.05	<0.1	
W_*hyg*	cot	none	hyg	151	0.55	5.46	1490±2%	6.2 ±0.2	0.11 / 0.67		
W_*ox*	cot	none	ox	170	0.53	n.d.	1352±2%	6.73 ±0.02	0.42 / 5.83		
W_*red*	cot	none	ox/red	170	0.53	n.d.	1431±1.1%	6.41 ±0.05	0.02		
W_G	cot	Gel+	none	170	0.54	6.13	3021±1%	5.70			
W_GI	cot	Gel+, I	none	170	0.62	6.90	2225*	4.21			
K	cot	Ca	none	100	0.68	5.61	2566±2%	8.89		7.6	7.3
W_*Ca*	cot	Ca	none	170	0.54	5.20	2803±2.2%	8.86		5.4	6.0
R	lin	none	none	160	0.54	5.78±0.18	2980	7.90			
R_*hyg*	lin	none	hyg	141	0.60	n.d.	1961±1.6%	6.14			
R_G	lin	Gel+	none	160	0.53	6.57	3326±6.8%	7.68			
R_GI	lin	Gel+, I	none	150	0.55	7.21	2290*	5.15			
SE	lin	Gel~	nat	115	0.64	5.46	1000±9.4%	5.90			
LN5	lin	Gel++	nat	125	0.62	5.36	1039±5.7%	4.92		1.1	
M	lin	Gel++	nat	125	0.47	5.75±0.04	1490±12.8%	5.03		1.5	
M_I	lin	Gel++, I	nat	125	0.72	n.d.	702*	n.d.			
LN1	lin	Gel+	nat	165	0.68	5.12	1608±2.3%	5.28		0.8	
DCN	lin	Gel~, Ca	nat	90	0.72	6.01	2869±6.2%	7.61		2.5	

X-ray radiation exposures

Synchrotron X-ray setup

The papers were cut into a few cm^2 samples, inserted in plastic photography slide frames, and heated for 2 h at 40 °C (Memmert UN 55 oven) for gentle moisture desorption. They were then placed 48 h in a climatic chamber at 23 °C and 50% RH for equilibrium moisture regain, after which they were sealed in LDPE plastic bags where silica gel ProSorb (Atlantis) was added so as to maintain 50% RH (± 5%). The EMC (23 °C, 50% RH) of the papers was determined according to the TAPPI test method (TAPPI T 502 cm-07 1998) (Table 1). No moisture leakage was recorded upon monitoring the RH inside the bags for at least 72 h prior to the synchrotron radiation (SR) experiment with a temperature/humidity logger (Ibutton® Hygrochron, Measurement Systems

Ltd). The bags were themselves sealed with Escal® film also filled with silica gel to stabilize the RH to 50% for transportation from the laboratory to the synchrotron facility.

The irradiation was performed on the beamline PUMA (SOLEIL synchrotron, Saclay). A monochromatic beam (2×1 cm^2) from a double crystal monochromator (DCM) with Si(111) crystals was used at photon energies of 7.22 keV, 12.5 keV or 18 keV. The samples were exposed perpendicular to the beam, inside the LDPE bags. The irradiation duration varied to reach various doses in the range 7 Gy to 4 kGy. The dose D (Gy), *i.e.* the total energy deposited per mass unit of material, was calculated as follows:

$$D = \frac{F \cdot E \cdot t}{m} = \frac{I_0 \cdot (1 - e^{-\mu x}) \cdot E \cdot t}{\rho \cdot \sigma \cdot x}$$

with F, the absorbed photon flux (ph s^{-1}) ; E, the energy of X-ray photons (J) ; t, the exposure time (s) ; I_0, the incident flux (ph s^{-1}) ; m, the mass of paper (kg) ; x, the thickness of paper (cm) ; ρ its density (g cm^{-3}) ; σ, the beam imprint ; μ the linear attenuation coefficient (cm^{-1}), which was determined by measuring the incident and transmitted flux impinging stacked sheets as previously described (Gimat et al. 2020).

Laboratory XRF spectrometer

W paper was irradiated using a Micro X-ray Fluorescence Spectrometer (M6 Jetstream, Brucker) with a 100 µm² polychromatic beam (0-50 keV). The beam is produced by an X-ray tube with a rhodium anode (50 kV, 600 µA). The instrument is equipped with a 100 µm-thick beryllium window and polycapillary optics are used to focus the X-ray beam. The X-ray detector is a 60 mm² SDD and has a Peltier cooler. For each energy of the X-ray source, the linear absorption coefficient μ was calculated using the coefficients, density and mass fraction of the most abundant components of paper, namely cellulose, water and air (Fig. S4 in the Supplementary data file).

The sample area was scanned in successive spots (area equal to the beam size) in one or repeated cycles. The signal to noise ratio of the XRF spectrum depends on the number of cycles and their duration. Two samples were thus exposed during 1 cycle for 500 ms and 3000 ms per spot and received doses of about 3.5 and 22 Gy, respectively. These doses were chosen to be in the same range as the two lowest doses used in the SR experiment at 7.22 keV (7 and 21 Gy). To study the dose-response reciprocity, one sample was exposed repeatedly for 30 cycles with 100 ms exposure per spot, thus being irradiated to 22 Gy.

Physico-chemical characterizations

After the irradiation, the samples were kept in the dark at 50% RH and 23 °C until analysis. The analyses were usually performed within 6 days, the latter being the shortest possible duration between the irradiation and the analysis. This allowed for immediate damage assessment. Post-irradiation monitoring was carried out by regularly re-examining the samples.

Molar masses

The molar mass distribution and the number- and weight-average molar masses of cellulose M_n and M_w were determined using Size-Exclusion Chromatography (SEC), except for the inked samples which were analyzed using viscometry. For SEC, paper samples (3-5 mg) were prepared and analyzed as described previously (Dupont 2003b). The precision on M_w was between 0.2 and 4.0 RSD%, depending on the samples.

S, the glycosidic scissions concentration, was calculated using DP_n, with $DP_n = \frac{M_n}{M_{AGU}} = \frac{N_{AGU}}{N_{molecule_t}}$, where N_{AGU} is the total number of anhydroglucose units, i.e monomers (M_{AGU} =162 g mol^{-1}) and $N_{molecule_t}$ is the total number of cellulose molecules at any time *t* (µmoles). As each glycosidic bond scission increases by one the number of cellulose chains, the increase in the concentration of new chains formed is equal to *S*. The number of scissions being equal to $N_{molecule_t} - N_{molecule_{t0}}$ and N_{AGU} being equal to 6170 µmol g^{-1} of paper, hence $S = 6170 \left(\frac{1}{DP_{n_t}} - \frac{1}{DP_{n_{t0}}}\right)$ µmoles g$^{-1}_{paper}$ (Whitmore and Bogaard 1994).

In order to avoid polluting the SEC columns with iron, *DP* of the gelatin-ink coated samples W_GI and R_GI was measured using viscometry in cupriethylene diamine (CED) (TAPPI T 230 om-19 1999) with a capillary viscometer Routine 100 (Cannon-Fenske). Irradiation was carried out four days after the ink application. Due to experimental constraints, the viscometry measurements were carried out 29 days after the irradiation. Before the viscometry analysis, the paper samples were chemically reduced with $NaBH_4$ (same treatment as described above) in order to avoid solvent induced depolymerization. They were dried between blotters and conditioned at 50% RH and 23 °C. The viscometric DP (DP_v) was calculated from the intrinsic viscosity [η] using the Mark-Houwink-Sakurada equation, by applying the coefficients proposed by Evans and Wallis (Evans and Wallis 1987) : $[\eta] = 0.91 \times DP_v^{0.85}$. DP_v is assumed to be very close to DP_w as M_v has been

reported to be closer from M_w than M_n (Ross-Murphy 1985). This allows to parallel DP_v with DP_w with some confidence. The formula proposed by Dupont et al. (Dupont et al. 2018) was used for the conversion of DP_v to DP_n: $DP_n = 1575\ e^{(DPw/3536)} - 1575$.

Hydroxyl radicals

The paper samples were soaked for 3 minutes in a methanolic solution of TPA (98%, Sigma Aldrich) (1 mM). They were left to dry at ambient temperature for 24 h and conditioned at 23 °C at 50% RH. TPA reacts with hydroxyl free radicals ($HO^{\bullet}$) in the paper and produces hydroxyterephthalic acid (HTPA), which accumulates in the paper. HTPA was extracted from the paper (2-3 mg) by soaking during three hours in 300 µl of phosphate buffer (KH_2PO_4 50 mM pH 3.2, 70% water:30% methanol), and was quantified by reverse phase liquid chromatography with UV and fluorescence detection (RP-HPLC/FLD-DAD) according to a previously established method (Jeong et al. 2014). HTPA (µmol g^{-1}) was calculated with respect to the paper dry weight, subtracting the additives weight, to correlate sample behavior based on their cellulosic content only. In order to ensure the quality of the results, it was verified that no HTPA was formed upon irradiating TPA powder.

Colorimetric and UV luminescence measurements

The diffuse reflectance and UV luminescence of the paper samples were measured with a non-invasive UV-Vis-NIR spectroradiometer (Specbos 1211UV, JETI). For UV luminescence, the excitation was centered at 365 nm (with full width half-maximum FWHM = 20 nm). Measurements were normalized to a blue luminescent certified reflectance standard (USFS-461 Spectralon) to correct for light intensity change with time. The maximum intensity of each UV luminescence spectrum was used to monitor the global intensity change. To calculate the change the following formula was used:

$$\Delta I(\lambda_{max}) = I(\lambda_{max})[irr] - I(\lambda_{max})[Ctrl]$$

with $I(\lambda_{max})[irr]$ and $I(\lambda_{max})[Ctrl]$ the intensities of luminescence at the wavelength maxima measured inside (irr) and outside (Ctrl) of the irradiated area, respectively.

A spectrophotometer (Konica Minolta, CM-26d) was used to measure the chromaticity coordinates L*, a* and b* in the CIELAB 1976 system. The variation of the color coordinate b^*,

285 which spans on the blue-yellow scale, was used to quantify the yellowing expressed as $\Delta b^* = b^* -$
286 b_0^* (positive value).
287

288 Results and discussion

289 *Calculation of the X-ray dose*

290 The extent of radiation damage usually depends on the X-ray dose absorbed by a sample. Different
291 papers are expected to absorb X-ray differently, especially when heavy elements are present as the
292 latter increase the absorption. Measuring the X-ray dose is thus essential in order to compare
293 changes in paper samples after irradiation on a common basis. In order to do so, it is necessary to
294 define the linear attenuation coefficient (μ) of each sample for each experimental setup and
295 condition (see synchrotron X-ray setup for dose calculation). μ depends on the sample material, but
296 also on the X- ray energy. For the laboratory instrument micro XRF irradiation, μ of the Whatman
297 n° 1 paper (W) was calculated using the entire energy spectrum of the polychromatic beam (Fig.
298 S4b in the Supplementary data file). For the experiments on PUMA beamline, the values of μ for
299 W were measured at the three energies used for the irradiation. The values decreased with
300 increasing energy: 4.29 ± 0.07 cm^{-1} at 7.22 keV, 1.02 ± 0.06 cm^{-1} at 12.5 keV and 0.31 ± 0.031 cm^{-}
301 ^{1} at 18 keV. The values for μ of the model and historical papers at 7.22 keV are given in Table 2.
302 Fe in W_GI and R_GI and the calcium carbonate in W_Ca and K both increase the photon
303 absorption. Although they contain a similar amount of calcium carbonate and have a similar pH
304 (~8.9), K has a higher μ than W_Ca. This value (9.56) was also the highest of all. This was
305 explained by the higher paper density as well as smaller and more homogeneously distributed
306 mineral particles. This observation also applies to the iron gallate ink coated papers, where the
307 presence of iron on the surface increases the value of μ. The gelatin in W_G seemed to increase
308 only slightly the value of μ, while the opposite was observed in R_G. The artificially aged samples
309 W_*hyg*, W_*ox*, W_*red* and R_*hyg* also showed a higher X-ray absorption, which might be due to
310 a slightly higher paper density.
311 The absorption coefficients of the archival paper samples varied from 5.60 (LN5) to 8.18 (DCN).
312 These values could again be related to the paper density, with the higher density papers DCN, MI
313 and LN1 exhibiting the higher μ values. The distribution of the fibers and non-fiber components

across the sheets also most probably played a role. DCN displayed the highest μ, which was attributed to the presence of calcium (Table 1), as well as copper and iron (Table 1, Table S1, Figs S3 & S5 in the Supplementary data file).

These results confirmed that the additives influenced the way paper absorbed X-rays and suggested that structural parameters such as fiber density may also play a role.

Table 2 Linear attenuation coefficient μ of Whatman n° 1 papers (cot), linen rag papers (lin) and archival papers (archiv) at 7.22 keV, 50% RH.

Model papers								
cot	W	W_*hyg*	W_*ox*	W_*red*	W_G	W_GI	K	W_Ca
μ (cm^{-1})	4.29±0.07	5.32±0.07	5.66±0.14	5.28±0.044	4.76±0.016	7.03±0.036	9.56±0.2	6.89±0.12
ρ (g cm^{-3})	0.51	0.55	0.53	0.53	0.54	0.62	0.68	0.54
lin	R	R_*hyg*			R_G	R_GI		
μ (cm^{-1})	5.01±0.25	5.69±0.28			4.77±0.07	7.99±0.08		
ρ (g cm^{-3})	0.54	0.6			0.53	0.55		
Archival papers								
archiv	SE	LN5	LN1	DCN	M	M_I		
μ (cm^{-1})	6.66±0.036	5.6±0.23	7.21±0.10	8.18±0.6	5.69±0.030	10.05±0.030		
ρ (g cm^{-3})	0.64	0.62	0.68	0.72	0.47	0.72		

DP and hydroxyl radicals

Impact of the X-ray dose and photon energy

A first experiment, carried out with a laboratory Micro X-ray Fluorescence Spectrometer, allowed assessing the impact of low doses in the range of those usually delivered by these laboratory instruments. All the unaged W samples, irradiated to a dose up to 22 Gy, had a similar *DP* to the Control sample (Fig. S6 in the Supplementary data file), indicating that no macromolecular degradation took place during the irradiation, whether the dose was delivered at once or in several stages. This is consistent with the lowest observable adverse effect dose (LOAED) for glycosidic scissions of 0.21 kGy defined in our previous work (Gimat et al. 2020).

Exposures to synchrotron X-ray radiation were carried out next to study (*i*) the variation of the photon energy and (*ii*) reach higher doses, similar to those used during spectroscopic examinations with this type of instrument. Synchrotron X-ray fluorescence experiments usually use energies in the range of 1 to 20 keV (Glaser and Deckers 2014), sometimes even higher if heavy elements are

investigated. To investigate if the degradation was energy dependent, W samples were exposed to three photon energies: 7.22, 12.5 and 18 keV. Fig. 1 shows the glycosidic scissions concentration (*S*) as a function of the absorbed dose up to 3.9 kGy, at the three energy levels. *S* increased with the dose in the range of 0 to 6 μmol g^{-1}. The impact was very small below the LOAED (0.21 kGy) and was followed by a linear increase from 0.5 kGy upwards. *S* increased steeply, similarly at 12.5 keV and 18 keV. At 7.22 keV, all the values of *S* were shifted up. A similar energy dependence has been observed for electron beam irradiation (Bouchard et al. 2006) at energies of several MeV. While the photoelectrons created by the X-ray photons in our experiment have much lower energies, it seems like the inverse relation between kinetic energy and cellulose damage remains true in the keV regime. We are not sure why this is the case, but it is noteworthy that the inelastic mean free path (IMFP) varies considerably for electron energies in the range of our experiment compared to the typical average diameter of cellulose fibers. The IMFP for electrons in graphite changes from 9.2 nm at 7.3 keV to 19.5 nm at 18 keV (Shinotsuka et al. 2015). While the exact path lengths in cellulose will likely be slightly different, this shows that it is thus much more probable that a photoelectron produced by 18 keV X-rays escapes the cellulose fibers before causing damage than it is for one produced by 7 keV X-rays. Based on these results, all the following experiments were carried out at 7.22 keV, the most penalizing conditions, to enhance the chances of observing and characterizing damage.

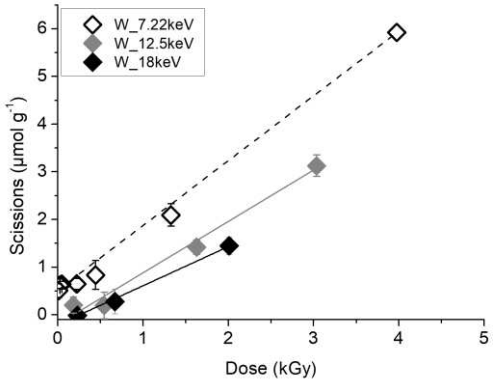

Fig. 1 Glycosidic scissions concentration *S* as a function of the X-ray dose in Whatman no. 1 irradiated at energy levels 7.22, 12.5 and 18 keV at 50% RH

Impact of calcium carbonate and gelatin

The glycosidic scissions and hydroxyl free radicals concentrations in the unaged papers, in the papers with calcium carbonate and in the papers with gelatin increased in a quasi linear fashion as a function of the X-ray dose, up to 6 μmol g^{-1} for W and up to 8 μmol g^{-1} for R (Figs. 2 & 3). *S* in W_G was slightly lower than in W Control (Fig. 2a). This observation is consistent with the fact that gelatin size tends to lower the depolymerization rate of cellulose during the degradation induced by aging (Dupont 2003a). Besides gelatin, this could also be partly due to the difference in moisture in unsized vs sized paper (EMC at 23◦C of 5.43% and 6.13%, respectively), as moisture was shown to reduce cellulose depolymerization during synchrotron X-ray irradiation (Gimat et al. 2020). Because ofa larger standard deviations on the data points, this was less clearly established for R and R_G, where *S* values were quasi similar (Fig. 2b) despite the EMC difference (5.78% vs 6.57%, respectively) (Table 1).

The samples with gelatin (W_G and R_G) produced less hydroxyl radicals than the Control samples (Fig. 3a and 3b). This could be an indication that gelatin was able to scavenge the HO° produced during the irradiation.

In both W_Ca and K, *S* increased slightly less as a function of the dose than in W Control, which is especially visible at the high doses, as shown on Fig. 2c. This suggests that calcium carbonate can buffer the acids produced during the X-ray exposure, which is the expected role of the alkaline reserve in paper (Whitmore and Bogaard 1994; Ahn et al. 2013; Rouchon and Belhadj 2016). On the other hand, W_Ca and K showed a larger HO° production than the Control samples (Fig. 3c). This, again, could be due to the pH, as an alkaline medium is known to enhance the lifetime of HO° radicals, and hence the probability that they react with TPA. These results also confirmed previous observations that the HO° concentration did not always correlate directly with the glycosidic scissions concentration, and indicate that other species and mechanisms are involved (Jeong et al. 2014; Gimat et al. 2020).

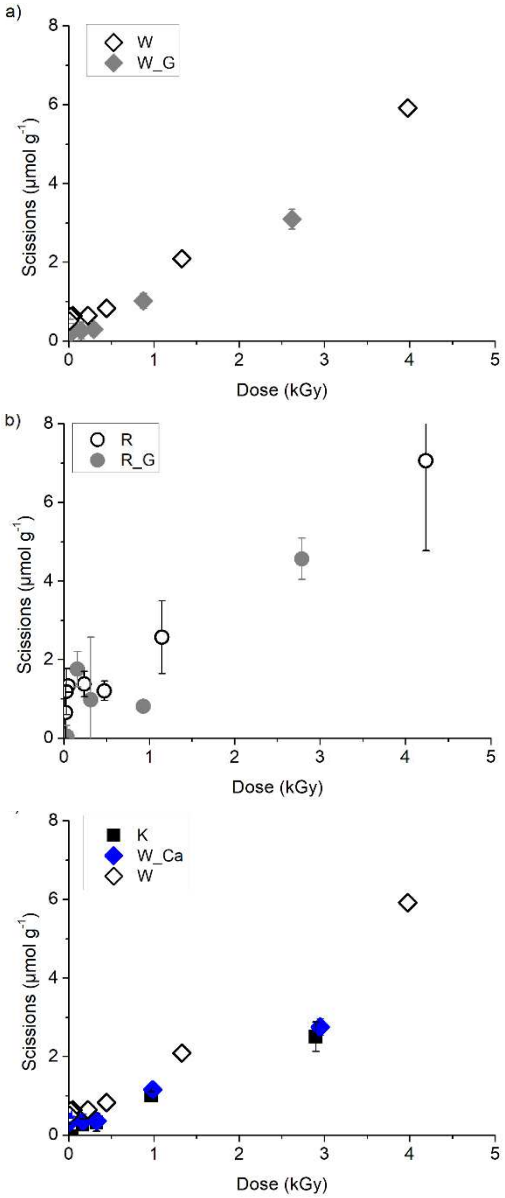

382

383

384 **Fig. 2** Glycosidic scissions concentration (*S*) in W and R Control papers, papers with gelatin (W_G and R_G) (a, b)
385 and with calcium carbonate (W_Ca and K) (c) as a function of X-ray dose.

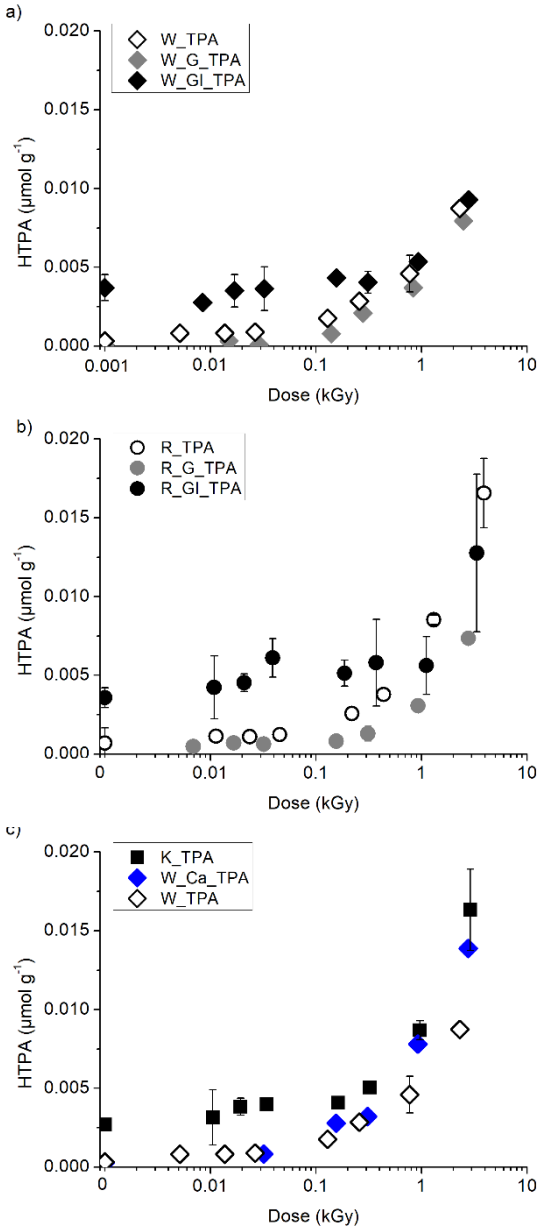

386

387 **Fig. 3** Impact of gelatin, iron gallate ink (a, b) and calcium carbonate (c) in W and R papers on the HTPA
388 concentration as a function of X-ray dose. The logarithmic scale is used for easier visualization.

389

390 Impact of the iron gallate ink

391 For the three samples coated with the iron gallate ink (W_GI, R_GI and M_GI), the *DP* of the non-
392 irradiated samples was considerably lower than that of the Control samples (W, R and M) as

represented by the arrows on Fig. 4. This was attributed to strong and almost instant acid hydrolysis and oxidation reactions due to the presence of iron gallate ink, which occurs within the period between sample preparation and analysis (33 days). This has been observed previously (Rouchon et al. 2011, 2016). Indeed, a *DP* loss of 25% and 30% was measured for W_GI and R_GI, respectively, which is consistent with previous observations (Rouchon et al. 2011) for inked Whatman n° 1 where a 24% *DP* loss was recorded within a similar timeframe. A striking observation was made in the low doses range: after irradiation (up to 0.29 kGy for W_GI, 0.36 kGy for R_GI and 2.4 kGy M_GI), the *DP* of the iron gallate ink coated samples was higher than the *DP* of their non-irradiated counterpart (Fig. 4, dashed lines). This was interpreted as having two possible causes. First, it has been shown that iron gallate ink containing papers produce free radicals, such as HO° and other reactive oxygen species (Gimat et al. 2016, 2017). This enhances the chances for free radicals recombination leading to the auto-oxidation termination reactions, and in turn lowers the concentration of radicals accumulated in the paper, thus, preserving cellulose from their attack. Secondly, the crosslinking induced by the recombination of cellulosic radicals could lead to an increase in *DP* which would be measurable if the radicals have high molar mass. This is consistent with the fact that in the low irradiation doses range, HTPA was produced in higher amount in the irradiated ink coated samples W_GI and R_GI than in the Control counterparts W and R (Fig. 3a, 3b), and in similar amount as in non-irradiated W_GI and R_GI. In the higher doses range (from 0.89 kGy for W_GI, 1.1 kGy for R_GI, and 6.3 kGy for M_GI), the samples reached a lower *DP* than the non-irradiated samples, and the HTPA concentration in the samples reached similar levels with and without ink. This was interpreted as an indication that the enhanced scissions induced by the irradiation at the high doses likely exceeded the supposed impact of the free radicals recombination reactions.

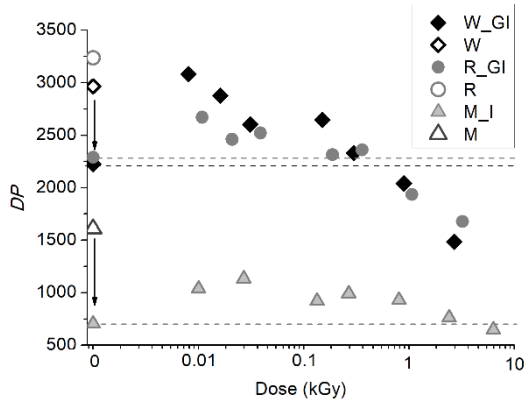

Fig. 4 Viscometric-average degree of polymerization (DP_v) of iron gallate ink coated papers W_GI (a), R_GI (b), and M_GI (c) as a function of X-ray dose (kGy). The dose is represented on a logarithmic scale for easier visualization. Control samples without ink or gelatin are represented by the void data points. Arrows represent the *DP* drop due to the iron gallate ink. At low X-ray doses, irradiated samples have a higher *DP* than non-irradiated control sample (above the dotted lines)

Impact of the degradation state

The artificially degraded papers (W_*hyg*, W_*ox* and W_*red*) were irradiated at 7.22 keV to various doses to study if and how the degradation state modifies the impact of the X-rays exposure. The intent was to possibly extrapolate the results to centuries-old cultural heritage paper. The three samples had a similar starting *DP* ($DP_w \approx 1400$, *i.e* about 50% lower than W) and a different oxidation state: $N_{Cu} = 0.42$ for W_*ox* (*i.e*. 5.83 µmol g^{-1} total carbonyl groups, as calculated according to (Röhrling et al. 2002), $N_{Cu} = 0.11$ for W_*hyg* (*i.e.* 0.67 µmol g^{-1} total carbonyl groups) and $N_{Cu} = 0.02$ for W_*red* (*i.e.* near-zero carbonyl groups besides the reducing ends) (Table 1). Figures 5a and 5b show the glycosidic scissions concentration in these samples as a function of the dose. In W_*hyg, S* increased linearly with the dose, yet slightly less than in W Control (Fig. 5a). This suggests that lower *DP* and/or higher carbonyl groups concentration might lessen somewhat the impact of X-rays (slight "counter-degradation effect"). For samples that underwent oxidation (W_*ox* and W_*red*), *S* was in the same range (up to 6 µmol g^{-1}) as for W and W_*hyg* at respective doses (Fig. 5b), yet with higher standard deviations. The main contrast between the two samples is in the low dose region. In the range –up to 0.5 kGy, while W_*red* underwent fewer glycosidic scissions, in W_*ox S* was higher than in the other samples, with a sharp increase to 1-2 µmol g^{-1} for

doses below 1.4 kGy. This indicates that at low doses, a high concentration of carbonyl groups in the paper tended to enhance the X-ray induced depolymerization. In the higher doses range (≥ 1 kGy), the depolymerization of all the samples reached the same range, between 4 and 6 μmol g^{-1}. The "carbonyl" ("pro-degradation") effect seemed overridden by the overall stronger depolymerization inflicted by the higher irradiation doses. Fig 6a shows that a similar amount of HO° free radicals was produced in W_*hyg* and in W, indicating that the free radicals were not fully responsible for the difference in the glycosidic scissions, and that the HO° were not significantly involved in the production of carbonyl groups.

Neither a pro-, nor a counter-degradation effect of low *DP* and high oxidation level was observed in the linen rag model papers. *S* extended higher (up to 8 μmol g^{-1}) and increased linearly as a function of the dose, yet, in a similar way for the undegraded Control sample and for the degraded R_*hyg*, despite the *DP* of the latter being 34% lower ($DP_w \approx 1961$) (Fig. 5c). Moreover, above 0.1 kGy, slightly less HO° free radicals were detected in R_*hyg* than in R (Fig. 6b). This, and the large standard deviations on each data point of R samples muddles the interpretations. The extrapolation of the results from a simple machine-made cellulosic paper to a traditional handmade rag pulp paper is not straightforward. The next level of complexity, which was to test the response of archival papers, was thus anticipated as very challenging.

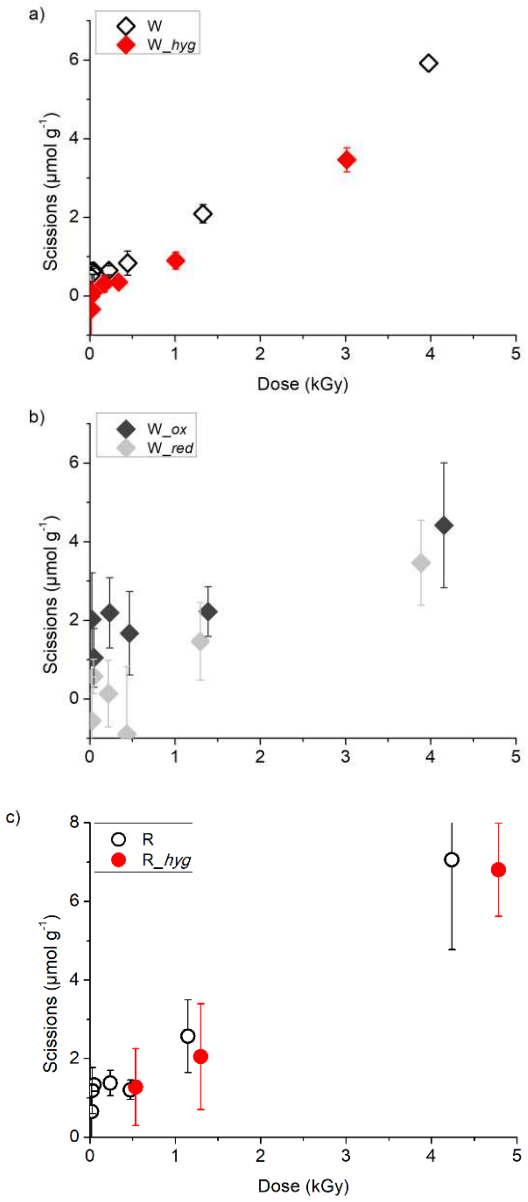

459 **Fig. 5** Glycosidic scissions concentration (*S*) in aged papers W (a, b) and aged rag papers *R* (c) as
460 a function of X-ray dose compared to respective control samples.

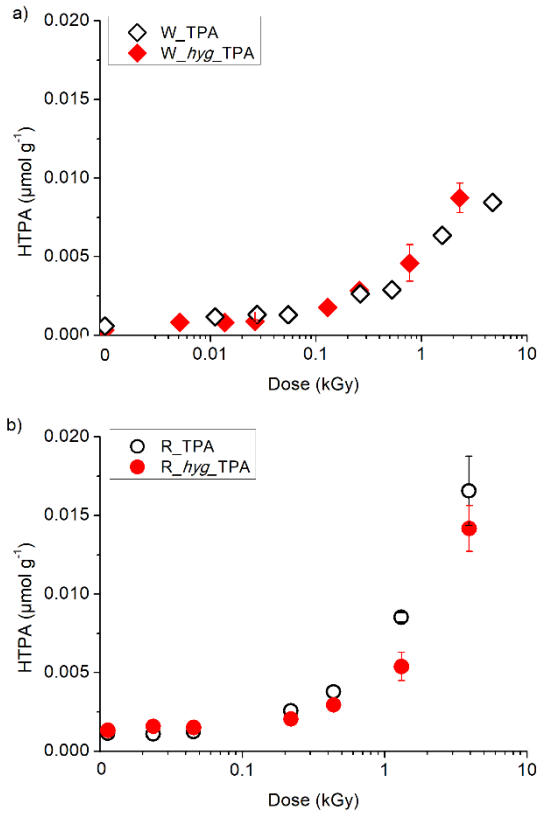

461 **Fig. 6** HTPA concentration in control samples, aged W (a) and aged *R* (b) as a function of X-ray
462 dose.
463

464 Archival paper documents

465 For the historic samples irradiated to various doses, *S* values were overall in the same range as
466 those measured for the model samples. Only LN5 degraded more and showed *S* values at least
467 twice as high at all the doses tested (Figs. 7a, 7b). However, the depolymerization behavior with
468 increasing dose was not progressive as observed for the model papers (except for LN1), especially
469 in the low doses. For instance, SE did not undergo scissions below 3 kGy, and M had a constant
470 degradation (plateau) response on the whole dose range, with *S* around 3.5 µmol g^{-1} (Fig. 7a). No
471 correlation could be made with the *DP* (table 1), the paper constituents or the paper density. All
472 the papers have similar iron and calcium content, except for DCN which has more calcium due to
473 the calcium carbonate filler (Fig. S5 in the Supplementary data file). The other possible difference
474 in composition would be the gelatin content, the latter being a factor that tends to lower the
475 degradation in the model papers. Unfortunately, the gelatin content of the archival papers was

476 unknown and could not be measured. However, an indirect indication of sizing was given by a
477 water drop absorption test, which showed that M and LN5 were more hydrophobic than DCN (fig.
478 S3 in the Supplementary data file). Even though there can be other reasons for paper
479 hydrophobicity such as reduced porosity for instance, the former two showed higher *S* then the
480 latter, which would tend to invalidate the aforementioned protective role of gelatin. The differences
481 in *S* could thus arise from local heterogeneity and to samples' structural parameters such as porosity
482 or constituents' composition. This was not unexpected as in handmade papers the additives are
483 usually not as homogeneously distributed at the microscopic level as in industrial papers.
484 Very high doses, between 32 and 38 kGy, were then tested on the archival papers, as well as on W.
485 The results showed that DCN, LN1 and LN5 were similarly extensively degraded as W, with *S*
486 comprised between 30 and 43 µmol g^{-1} (Figs 7a & 7b). M and SE resisted surprisingly well, being
487 the least degraded samples, with *S* close to 10 µmol g^{-1}. Despite the different kinetics, most samples
488 approached LODP (Levelling Off Degree of Polymerization) with DP_w W = 345; DP_w M =318;
489 DP_w LN5= 426; DP_w LN1= 495. The least degraded samples were DCN (DP_w = 530) and SE (DP_w
490 = 708) (Fig. 7c). The production of HO° free radicals was measured in SE and M. In SE, HO°
491 concentration was very low, but it was higher in M over the whole dose range reaching a similar
492 amount as in the model papers containing Ca and ink (Fig. 7d). This difference was thus attributed
493 to the slightly higher calcium and iron content in M than in SE (Fig. S5 in the Supplementary data
494 file).

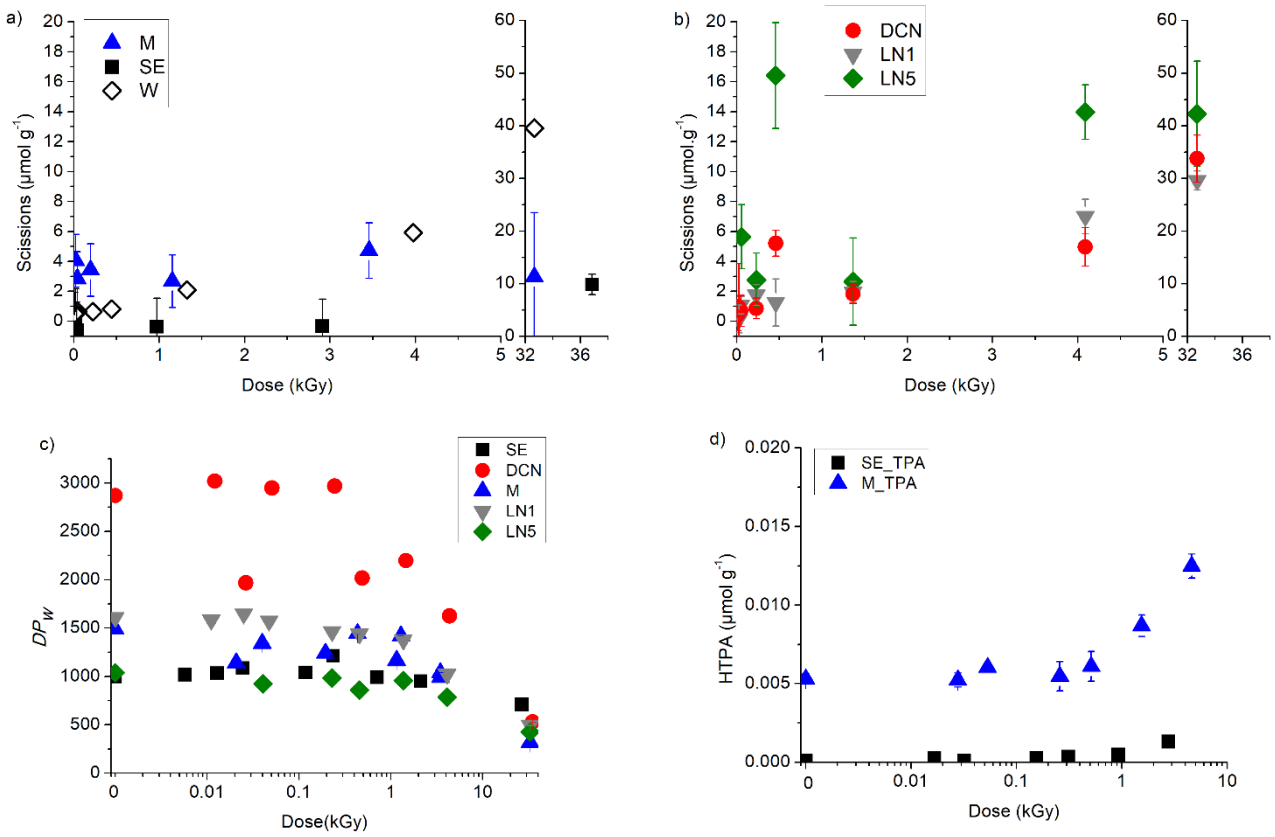

Fig. 7 Glycosidic scissions concentration (*S*) (a, b), DP_w (c) and HTPA concentration (d) in archival samples as a function of X-ray dose. Logarithmic scale (c-d) is used only for a better display of the data.

UV Luminescence and yellowing

Before the irradiation, all the samples, model and archival papers, exhibited luminescence under UV when excited at 365 nm, which is a common feature of paper (Fig. S7 in the Supplementary data file). The model samples W and R exhibited a luminescence maximum λ_{max} at 432 nm, which is consistent with previous data (Gimat et al. 2020). The intensity varied depending on the degradation state, luminophores being produced during the aging, and on the type of additive. For instance gelatin is expected to show a broad luminescence spectrum with λ_{max} = 402 nm (unaged) and 414 nm (artificially aged at 50% RH and 80° C) (Yova et al. 2001; Duconseille et al. 2016). After X-ray exposure, no change in the UV luminescence spectral distribution was observed during the three years monitoring period. The intensity at λ_{max} [$I(\lambda_{max})$] of each spectrum was followed

over time. After eight months, the area irradiated at 7.22 keV of the model papers (dose range from 2.8 to 4 kGy, depending on the sample) exhibited an increase in the intensity of the UV luminescence compared to the respective Control samples ($\Delta I(\lambda_{max})$), as shown Fig. 8 and Fig. S8 (Supplementary data file). All Whatman no.1 model papers (except for the sized samples), showed luminescence proportionally to the absorbed dose (Fig 8, white marks, linear trendline). The highest increase in luminescence was observed on the sized samples W_G and R_G with $\Delta I(\lambda_{max})$R_G of 0.0042 and $\Delta I(\lambda_{max})$W_G of 0.0036 (R_G data not shown), indicating that a large quantity of luminophores was produced post-irradiation. These samples were still the most luminescent samples after 11 months. The luminescence of W_*hyg* and K grew beyond that of the other samples between 8 and 11 months. The change in luminescence between unaged and aged R papers (with no additives) was slower than for unaged and aged W, with a smaller $\Delta I(\lambda_{max})$ of R and R_*hyg* (0.0011 and 0.00015, respectively) compared to W and W_*hyg* ($\Delta I(\lambda_{max})$ (0.0022 and 0.0025, respectively).

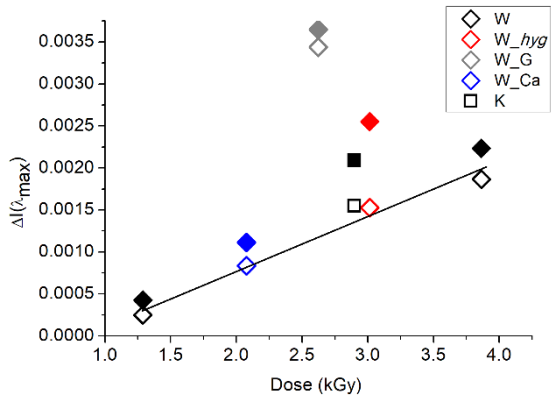

Fig. 8 $\Delta I(\lambda_{max})$ of W, 8 months (empty marks) and 11 months (full marks) after X-ray irradiation. $\Delta I(\lambda_{max})$ is the subtraction of the luminescence of the non-irradiated area from that of the irradiated area. The black trendline represents the dose/luminescence response in W Ctrl samples.

Colorimetric measurements were carried out three years after the irradiation, on the irradiated areas and the non-irradiated control samples (Fig. 9). All the model samples showed very small Δb^* values (Fig. 10a) and a global color change ΔE^* between 0.55 (for K) and 1.87 (for R), i.e. below the usually accepted level for a just noticeable difference. Among the W samples, the artificially aged W_*hyg* had the highest Δb^* (1.35 ± 0.26). The opposite trend was observed with R samples, where R_*hyg* had a lower Δb^* than R. This observed behavior difference is all the more valid since

the data points for R on Fig 10a correspond to higher doses than for W samples and that R_*hyg* is the most strongly irradiated sample. This may indicate complex radiochemistry mechanisms of chromophore destruction and chromogens formation. As opposed to the observations after hygrothermal aging of gelatin sized papers (Dupont 2003a; Missori et al. 2006), the irradiation did not modify the yellowing in the gelatin sized papers. This may be related to the radical scavenging properties of gelatin, which could lower the kinetics of cellulose chromophores formation. To sum up, for the model samples, the additive that had the highest impact on luminescence was gelatin. This is most probably due to its own intrinsic luminescence properties and to maybe also to its chromogenic degradation products appearing post-irradiation. Yellowing did not appear to be linked to either the initial conservation state nor to the presence of additives, which indicates complex mechanisms at play of chromogenic structure formation and destruction.

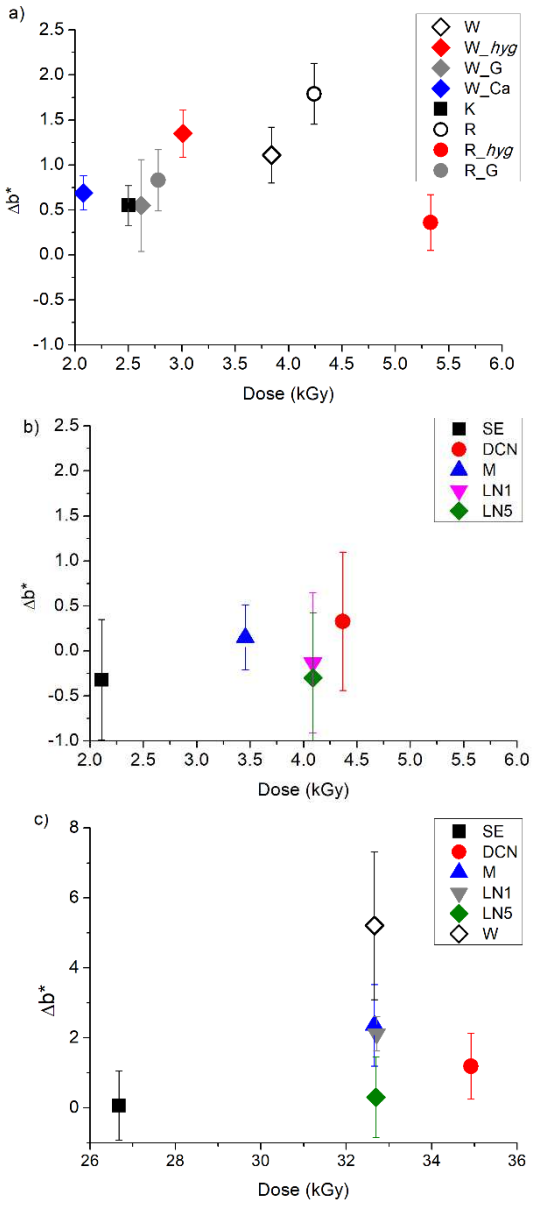

Fig. 9 Yellowing increase (Δb*) of papers measured three years after X-ray irradiation on W and R model papers (a) and on the archival papers (b, c).

The initial UV luminescence spectra of the archival papers showed maxima with different intensities I(λ_{max}) and positions (between 444 nm and 460 nm), which could be due to differences in the quantity and the type of UV-absorbing groups such as carbonyl compounds, respectively. This could also be due to a different moisture content, as the latter has been shown to affect the luminescence properties of paper (Kocar et al. 2005; Castellan et al. 2007). Before irradiation, no

correlation between the state of degradation (*DP*) and the intensity of the luminescence of the papers could be made. Indeed, LN1 and M, both with similar *DP* around 1500, displayed more intense luminescence than the other historic samples, either more degraded (DP_w LN5 = 1039 ± 5.7%, and *DP* SE =1000 ± 9.4%) or less degraded (*DP* DCN = 2869 ± 6.2%).The presence of additives such as gelatin could not be fully responsible of the luminescence intensity either, as the latter was not correlated to the hydrophobic properties used as an indication of the gelatin content (M and LN5 highly hydrophobic, LN1 medium hydrophobic, SE and DCN not hydrophobic)

After irradiation at doses below 4.4 kGy no change was observed on the archival papers. Indeed, no differences in the UV luminescence (data not shown) nor the yellowing ($\Delta b^* < 1$) were measured in the irradiated vs the non-irradiated areas (Fig. 9b). At the highest doses tested (26-36 kGy), a slight luminescence appeared on M and DCN twenty-one months after the irradiation (Fig. 10). It thus took almost two years for the luminophores to build up inside the archival papers. Similarly, as with the model samples, no correlation between the luminescence and the *DP*, or the glycosidic scissions could be made. A test was made by irradiating M at a very high dose (290 kGy), which induced marginal luminescence, and only after ten months (data not shown).

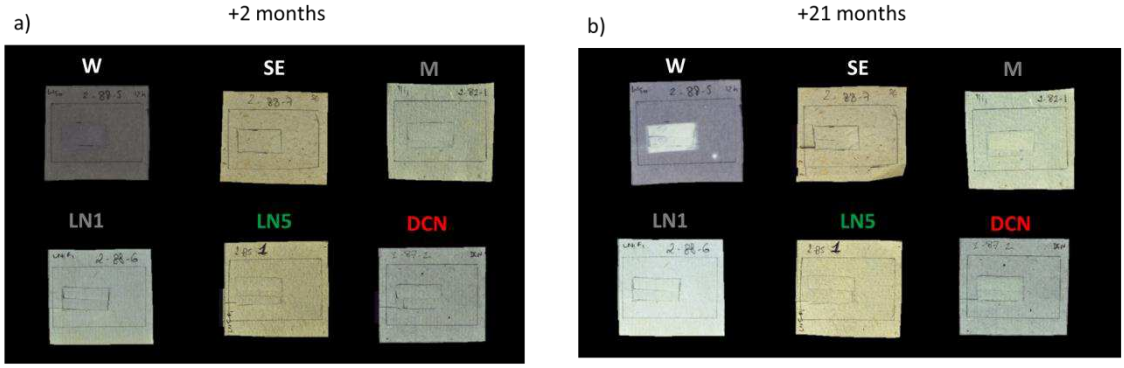

Fig. 10 Photographs under UV light of W and archival papers exposed to X-ray radiation at doses between 26 and 33 kGy, 1 month (a) and 21 months (b) after the irradiation.

Within the high dose range (26-36 kGy), no change was observed for SE and LN5, and the other archival samples (DCN, M, LN1) exhibited a slight yellowing, with Δb^* of 1.2, 2.4, and 2.1, respectively (Fig.9c). The strongest yellowing was recorded on W ($\Delta b^* = 5.2 \pm 2.1$) .

In conclusion, the behavior of historical papers under X-ray is multifactorial and difficult to predict. This study showed that the response of archival paper to X-ray radiation is very varied, in

terms of *DP* losses (the largest being for DCN and LN1), luminescence (M and DCN exhibited the higher luminescence intensity), and yellowing (M and LN1 yellowed the most). These observations led to the conclusion that in the samples with additives and in the aged/degraded samples, optical changes (yellowing and luminescence) were mostly uncorrelated. Moreover, as observed with the model papers, these optical changes were also not directly correlated with the macromolecular state (depolymerization). These observations underline the complex chemistry triggered by the exposure to X-rays.

Conclusion

Synchrotron X-ray radiation at energies and doses most often applied for analytical purposes to paper-based cultural heritage has been shown to be detrimental to one-component cellulosic paper (Whatman n°1). However, field situations are complex as historic papers are multiparametric, which interferes with a precise prediction of the effect of X-ray radiation. They usually are degraded to some extent and they contain other constituents besides the biopolymers, such as papermaking additives, ink and their degradation by-products. The present research investigated how these parameters could influence the X-ray radiation-induced degradation when studied separately in model papers. The latter were artificially aged and/or supplemented with additives, which enabled to single out some of the influential parameters. The additives tested were gelatin as sizing agent, and calcium carbonate as filler. Iron gallate ink was applied on some of the gelatin-sized papers, modeling writing/drawing medium. Following the same methodological approach as developed in a previous publication (Gimat et al 2020), the changes were measured immediately after the irradiation at the microscopic level (macromolecular and molecular degradation) and the macroscopic changes embodied by the optical properties (UV luminescence and yellowing) were monitored time-delayed.

In the dose range from 0 to 4 kGy, gelatin-sized samples and samples with $CaCO_3$ underwent a slightly reduced irradiation-induced depolymerization. Surprisingly, up to 0.89-1.1 kGy, the iron gallate ink coated papers had a higher *DP* than the Control samples, which was attributed to a decrease in the free radical initiated autooxidation reactions through radicals recombination and crosslinking. Above these doses, a higher rate of scissions induced by the irradiation prevailed. The production of hydroxyl free radicals was higher in all the samples containing $CaCO_3$, maybe due

609 to the increased lifetime of HO° at alkaline pH. The depolymerization behavior of the aged model
610 samples was different in the industrially-made (Whatman no 1) and in the handmade papers (linen
611 rags). Higher degradation state (lower *DP*) tended to stabilize Whatman n°1 paper towards X-ray
612 radiation, by lowering the macromolecular degradation. Conversely, the aged handmade paper
613 showed a similar amount of glycosidic scissions as the unaged counterpart. Carbonyl groups in the
614 artificially aged Whatman n°1 papers increased the glycosidic scissions in the low doses range,
615 below 0.5 kGy. Confirming previous results (Gimat et al. 2020), the optical changes appeared with
616 considerable delay, often one year after the irradiation, and could not be directly correlated to the
617 initial *DP* nor to the glycosidic scissions concentration that grew steadily during this post-
618 irradiation period (dark storage, room temperature). As expected, the archival papers made of linen
619 rags had an overall more complex X-ray exposure behavior than the model papers. First, the *DP*
620 was roughly constant in the low doses range below 4 kGy, which led us to increase the irradiation
621 doses. The large dispersion of the data was attributed to the paper macroscopic and microscopic
622 heterogeneity in terms of additives distribution degradation state and microstructure, but also to
623 the presence of multiple possible pro- and counter-degradation constituents in historic papers acting
624 synergistically. At very high doses (26-36 kGy), the archival papers reached the LODP
625 immediately upon irradiation, similarly as Whatman n° 1. No color change or UV luminescence
626 were observed within one year after the exposure at those high doses. After twenty-one months,
627 two archival papers showed a slight UV luminescence, but no clear connection with the
628 depolymerization or with the constituents could be made. These contrasted results indicate that
629 laboratory samples have their limitations to model archival/historic papers and that the
630 radiochemistry at play is rather complex. However, the observation that, overall, the historic papers
631 resisted better the X-ray exposures than modern papers is an important step forward that enables
632 to consider analyzing historic papers with better confidence. This work focused on the paper
633 material in chemical terms. Considering paper microstructure properties in the future may shed
634 more light on the limitations encountered.
635 A significant outcome of this work was to show the importance of carefully choosing the analytical
636 conditions that limit the exposure, thus the dose, when analyzing genuine artefacts using X-rays.
637 This can be achieved either by applying higher energy, or using low exposure times, and always
638 maintaining some humidity, as demonstrated in our previous work. The mid-range relative
639 humidity value recommended for paper-based cultural heritage storage is thus a good compromise.

Documenting the exact location of the X-ray photons impact and implementing a long-term monitoring of the eventual changes through regular photographic follow-up under both UV and visible lights are also advisable.

Acknowledgements

This research was supported by Paris Seine Graduate School of Humanities, Creation, Heritage, Investissements d'Avenir ANR-17-EURE-0021-Foundation for Cultural Heritage Science. We are grateful to synchrotron Soleil for the access to the PUMA beamline within the proposal 20181723 and to Tülin Okbinoglu for her help on the beamline. We thank Samia Rebaa and Naomi Nganzami Ebale, undergraduate chemistry students (Sorbonne Université), for help with photography and spectroscopy. We also thank Sabrina Paris Lacombe for technical help with Size Exclusion Chromatography.

References

Ahn K, Banik G, Potthast A (2012) Sustainability of Mass-Deacidification. Part II: Evaluation of Alkaline Reserve. Restaurator International Journal for the Preservation of Library and Archival Material 33:48–75. https://doi.org/10.1515/res-2012-0003

Ahn K, Rosenau T, Potthast A (2013) The influence of alkaline reserve on the aging behavior of book papers. Cellulose 20:1989–2001. https://doi.org/10.1007/s10570-013-9978-3

Albertin F, Astolfo A, Stampanoni M, et al (2015) Ancient administrative handwritten documents: X-ray analysis and imaging. J Synchrotron Radiat 22:446–451. https://doi.org/10.1107/S1600577515000314

Barrett T (1992) Evaluating the effect of gelatin sizing with regard to the permanence of paper. In: The Institute of Paper Conservation: conference papers Manchester 1992. Institute of paper conservation, Manchester, pp 228–233

Barrow WJ (1972) Manuscripts and Documents: Their Deterioration and Restoration. University Press of Virginia

Bertrand L, Schöeder S, Anglos D, et al (2015) Mitigation strategies for radiation damage in the analysis of ancient materials. TrAC Trends in Analytical Chemistry 66:128–145. https://doi.org/10.1016/j.trac.2014.10.005

671 Bicchieri M, Monti M, Piantanida G, Sodo A (2016) Effects of gamma irradiation on deteriorated
672 paper. Radiation Physics and Chemistry 125:21–26.
673 https://doi.org/10.1016/j.radphyschem.2016.03.005

674 Bouchard J, Méthot M, Jordan B (2006) The effects of ionizing radiation on the cellulose of
675 woodfree paper. Cellulose 13:601–610. https://doi.org/10.1007/s10570-005-9033-0

676 Castellan A, Ruggiero R, Frollini E, et al (2007) Studies on fluorescence of cellulosics.
677 Holzforschung 61:504–508. https://doi.org/10.1515/HF.2007.090

678 Creagh D (2007) Chapter 1 Synchrotron Radiation and its Use in Art, Archaeometry, and
679 Cultural Heritage Studies. In: Physical Techniques in the Study of Art, Archaeology and
680 Cultural Heritage. Elsevier, Amsterdam, pp 1–95

681 Duconseille A, Andueza D, Picard F, et al (2016) Molecular changes in gelatin aging observed by
682 NIR and fluorescence spectroscopy. Food Hydrocolloids 61:496–503.
683 https://doi.org/10.1016/j.foodhyd.2016.06.007

684 Dupont A-L (2003a) Gelatine sizing of paper and its impact on the degradation of cellulose
685 during ageing. Universiteit van Amsterdam

686 Dupont A-L (2003b) Cellulose in lithium chloride/N,N-dimethylacetamide, optimisation of a
687 dissolution method using paper substrates and stability of the solutions. Polymer
688 44:4117–4126. https://doi.org/10.1016/S0032-3861(03)00398-7

689 Dupont A-L, Réau D, Bégin P, et al (2018) Accurate molar masses of cellulose for the
690 determination of degradation rates in complex paper samples. Carbohydrate Polymers
691 202:172–185. https://doi.org/10.1016/j.carbpol.2018.08.134

692 Emery JA, Schroeder HA (1974) Iron-catalyzed oxidation of wood carbohydrates. Wood Science
693 and Technology 8:123–137. https://doi.org/10.1007/BF00351367

694 Ershov BG (1998) Radiation-chemical degradation of cellulose and other polysaccharides.
695 Russian Chemical Reviews 67:315–334

696 Evans R, Wallis AFA (1987) Comparison of cellulose molecular weights determined by high
697 performance size exclusion chromatography and spectrometry

698 Gervais C, Thoury M, Réguer S, et al (2015) Radiation damages during synchrotron X-ray micro-
699 analyses of Prussian blue and zinc white historic paintings: detection, mitigation and
700 integration. Appl Phys A 121:949–955. https://doi.org/10.1007/s00339-015-9462-z

701 Gimat A (2016) Comprehension of cellulose depolymerisation mechanisms induced by iron ions.
702 Université Pierre et Marie Curie

703 Gimat A, Dupont A-L, Lauron-Pernot H, et al (2017) Behavior of cellobiose in iron-containing
704 solutions: towards a better understanding of the dominant mechanism of degradation of

cellulosic paper by iron gall inks. Cellulose 24:5101–5115. https://doi.org/10.1007/s10570-017-1434-3

Gimat A, Kasneryk V, Dupont A-L, et al (2016) Investigating the DMPO-formate spin trapping method for the study of paper iron gall ink corrosion. New J Chem 40:9098–9110. https://doi.org/10.1039/C6NJ01480A

Gimat A, Schöder S, Thoury M, et al (2020) Short- and Long-Term Effects of X-ray Synchrotron Radiation on Cotton Paper. Biomacromolecules 21:2795–2807. https://doi.org/10.1021/acs.biomac.0c00512

Glaser L, Deckers D (2014) The Basics of Fast-scanning XRF Element Mapping for Iron-gall Ink Palimpsests. Manuscript cultures 7:104–112

Henniges U, Hasani M, Potthast A, et al (2013) Electron Beam Irradiation of Cellulosic Materials—Opportunities and Limitations. Materials 6:1584–1598. https://doi.org/10.3390/ma6051584

IAEA (2016) Trends of Synchrotron Radiation Applications in Cultural Heritage, Forensics and Materials Science. INTERNATIONAL ATOMIC ENERGY AGENCY, Vienna

Jeong M-J, Dupont A-L, de la Rie ER (2014) Degradation of cellulose at the wet–dry interface. II. Study of oxidation reactions and effect of antioxidants. Carbohydrate Polymers 101:671–683. https://doi.org/10.1016/j.carbpol.2013.09.080

Kabacińska Z, Yate L, Wencka M, et al (2017) Nanoscale Effects of Radiation (UV, X-ray, and γ) on Calcite Surfaces: Implications for its Mechanical and Physico-Chemical Properties

Kocar D, Strlic M, Kolar J, et al (2005) Chemiluminescence from paper III: the effect of superoxide anion and water. Polym Degrad Stabil 88:407–414. https://doi.org/10.1016/j.polymdegradstab.2004.12.005

Kozachuk M, Suda A, Ellis L, et al (2016) Possible Radiation-Induced Damage to the Molecular Structure of Wooden Artifacts Due to Micro-Computed Tomography, Handheld X-Ray Fluorescence, and X-Ray Photoelectron Spectroscopic Techniques. Journal of Conservation and Museum Studies 14:2–6. https://doi.org/10.5334/jcms.126

Mantler M, Klikovits J (2004) Analysis of art objects and other delicate samples: Is XRF really nondestructive? Powder Diffraction 19:16–19. https://doi.org/10.1154/1.1649962

Missori M, Righini M, Dupont A-L (2006) Gelatine sizing and discoloration: A comparative study of optical spectra obtained from ancient and artificially aged modern papers. Optics Communications 263:289–294. https://doi.org/10.1016/j.optcom.2006.02.004

Moini M, Rollman CM, Bertrand L (2014) Assessing the Impact of Synchrotron X-ray Irradiation on Proteinaceous Specimens at Macro and Molecular Levels. Anal Chem 86:9417–9422. https://doi.org/10.1021/ac502854d

Nevell TP, Zeronian S (1985) Cellulose Chemistry and its Applications. Prentice Hall

Poggi G, Sistach MC, Marin E, et al (2016) Calcium hydroxide nanoparticles in hydroalcoholic gelatin solutions (GeolNan) for the deacidification and strengthening of papers containing iron gall ink. Journal of Cultural Heritage 18:250–257. https://doi.org/10.1016/j.culher.2015.10.005

Potthast A, Henniges U, Banik G (2008) Iron gall ink-induced corrosion of cellulose: aging, degradation and stabilization. Part 1: model paper studies. Cellulose 15:849–859. https://doi.org/10.1007/s10570-008-9237-1

Pouyet E, Devine S, Grafakos T, et al (2017) Revealing the biography of a hidden medieval manuscript using synchrotron and conventional imaging techniques. Analytica Chimica Acta 982:20–30. https://doi.org/10.1016/j.aca.2017.06.016

Reissland B (1999) Ink Corrosion Aqueous and Non Aqueous Treatment of Paper Objects - State of the Art. Restaurator 20:167–180

Röhrling J, Potthast A, Rosenau T, et al (2002) A Novel Method for the Determination of Carbonyl Groups in Cellulosics by Fluorescence Labeling. 2. Validation and Applications. Biomacromolecules 3:969–975. https://doi.org/10.1021/bm020030p

Ross-Murphy SB (1985) Properties and uses of cellulose solutions. Chapter 8. In: Nevell TP, Zeronian S (eds) Cellulose Chemistry and its Applications, Wiley. Prentice Hall, New York, pp 202–222

Rouchon V, Belhadj O (2016) Calcium Hydrogen Carbonate (Bicarbonate) Deacidification: What you always wanted to know but never dared asking. Journal of Paper Conservation 17:125–127. https://doi.org/10.1080/18680860.2016.1287406

Rouchon V, Belhadj O, Duranton M, et al (2016) Application of Arrhenius law to DP and zero-span tensile strength measurements taken on iron gall ink impregnated papers: relevance of artificial ageing protocols. Appl Phys A 122:773. https://doi.org/10.1007/s00339-016-0307-1

Rouchon V, Duranton M, Burgaud C, et al (2011) Room-Temperature Study of Iron Gall Ink Impregnated Paper Degradation under Various Oxygen and Humidity Conditions: Time-Dependent Monitoring by Viscosity and X-ray Absorption Near-Edge Spectrometry Measurements. Anal Chem 83:2589–2597. https://doi.org/10.1021/ac1029242

Selih VS, Strlic M, Kolar J, Pihlar B (2007) The role of transition metals in oxidative degradation of cellulose. Polym Degrad Stabil 92:1476–1481. https://doi.org/10.1016/j.polymdegradstab.2007.05.006

Sequeira S, Casanova C, Cabrita EJ (2006) Deacidification of paper using dispersions of Ca(OH)2 nanoparticles in isopropanol. Study of efficiency. Journal of Cultural Heritage 7:264–272. https://doi.org/10.1016/j.culher.2006.04.004

776 Shinotsuka H, Tanuma S, Powell CJ, Penn DR (2015) Calculations of electron inelastic mean
777 free paths. X. Data for 41 elemental solids over the 50 eV to 200 keV range with the
778 relativistic full Penn algorithm. Surface and Interface Analysis 47:1132–1132.
779 https://doi.org/10.1002/sia.5861

780 TAPPI - T 430 cm-99 (1999) Copper Number of Pulp, Paper, and Paperboard

781 TAPPI 211 om-02 (2002) Ash in wood, pulp, paper and paperboard: combustion at 525°C

782 TAPPI T 230 om-19 (1999) Viscosity of pulp (capillary viscometer method), Test Method
783 TAPPI/ANSI T 230 om-19

784 TAPPI T 402 sp-08 (2013) Standard conditioning and testing atmospheres for paper, board, pulp
785 handsheets, and related products

786 TAPPI T 502 cm-07 (1998) Equilibrium relative humidity of paper and paperboard, Test Method
787 T 502 cm-07

788 TAPPI T 509 om-15 (2002) Hydrogen ion concentration (pH) of paper extracts (cold extraction
789 method), Test Method T 509 om-15

790 TAPPI T 553 om-00 (2000) Alkalinity of paper as calcium carbonate (alkaline reserve of paper)

791 TAPPI T573 sp-15 (2015) Accelerated temperature aging of printing and writing paper by dry
792 oven exposure apparatus

793 Whitmore PM, Bogaard J (1994) Determination of the Cellulose Scission Route in the Hydrolytic
794 and Oxidative Degradation of Paper. Restaurator 15:26–45.
795 https://doi.org/10.1515/rest.1994.15.1.26

796 Yova D, Hovhannisyan V, Theodossiou T (2001) Photochemical effects and hypericin
797 photosensitized processes in collagen. Journal of biomedical optics 6:52–7.
798 https://doi.org/10.1117/1.1331559

799

Supplementary Files

This is a list of supplementary files associated with this preprint. Click to download.

- GimatXrayadditiveSupplementarydata.docx